AN EXPERIMENTAL STUDY ON LI-ION BATTERY PERFORMANCE FOR SECOND LIFE APPLICATIONS AFTER DEGRADATION

BARAN KILIÇÇIOĞLU

ÖZYEĞİN UNIVERSITY

FEBRUARY, 2025

AN EXPERIMENTAL STUDY ON LI-ION BATTERY PERFORMANCE FOR SECOND LIFE APPLICATIONS AFTER DEGRADATION

by

BARAN KILIÇÇIOĞLU

Thesis
Submitted in Partial Fulfillment of the
Requirements for the Degree of

Master of Science

in
Electrical and Electronics Engineering

Advisor: Asst. Prof. Göktürk Poyrazoğlu
Co-Advisor: Dr. Hamza Makhamreh

Graduate School of Science and Engineering
Özyeğin University
İstanbul

FEBRUARY, 2025

AN EXPERIMENTAL STUDY ON LI-ION BATTERY PERFORMANCE FOR SECOND LIFE APPLICATIONS AFTER DEGRADATION

Approved by:

Asst. Prof. Göktürk Poyrazoğlu, Advisor
Department of Electrical & Electronics Engineering
Özyeğin University

Prof. Dr. Serkan Topaloğlu
Department of Electrical & Electronics Engineering
Yeditepe University

Asst. Prof. Umut Başaran
Department of Electrical & Electronics Engineering
Özyeğin University

Approval Date: December 26, 2024

To those who supported and encouraged me throughout this journey...

DECLARATION OF ORIGINALITY

I hereby declare that I am the sole author of this thesis and that this is the true copy of my thesis, including the final revisions, approved by my thesis committee. All data and information have been obtained, produced, and presented in accordance with the rules of research ethics and principles of academic honesty. As required by these rules, to the best of my knowledge I have acknowledged ideas, thoughts, and any copyrighted material in accordance with the standard referencing rules. I certify that any part of this thesis has not been submitted for a degree or diploma in another educational institution.

Baran KILIÇÇIOĞLU

ABSTRACT

This thesis investigates the second-life framework potential of lithium-ion cells, emphasizing non-invasive approaches and state of health State of Health (SoH) modeling. The study begins with an analysis of the first life of batteries, covering manufacturing processes and the factors that determine their readiness for second-life applications. Battery assemblies are categorized into two groups: permanently connected systems, such as laser-welded or ultrasonically bonded, and non-permanent systems, such as bolted connections or mechanically secured cell beds. Non-permanent assemblies are identified as the most suitable for second-life applications, forming the foundation of a second-life framework. To support this framework, efficient SoH estimation methods are developed and validated. Two models are proposed: a detailed model incorporating cycling conditions, charge rates, and depth of discharge Depth of Discharge (DoD), and a simpler model focusing on changes in DC internal resistance Direct Current Internal Resistance (DCIR)(%) value and cycle count. Both models demonstrate reliable SoH predictions, facilitating the effective sorting and reuse of cells without permanent interconnections. While the detailed model provides greater insights into cell aging, the simpler model offers practical advantages with lower testing requirements, making it suitable for scalable second-life applications. By validating these models under varied conditions, the study contributes to second-life methodologies by presenting adaptable, non-invasive estimation tools and scalable solutions for battery reuse.

Keywords: Li-Ion Batteries, second life, state of health (SoH), depth of discharge (DoD), parameter estimation–

ÖZET

Bu tez, lityum-iyon bataryalarının/hücrelerinin ikinci yaşam çerçevesi potansiyelini, invaziv olmayan yaklaşımlar ve SoH modellemesine odaklanarak incelemektedir. Çalışma, bataryaların birinci yaşamına ilişkin bir analizle başlamış, üretim süreçleri ve ikinci yaşam uygulamaları için uygunluklarını belirleyen faktörleri ele almıştır. Batarya düzenekleri, kalıcı bağlantılı sistemler (ör. lazer kaynaklı veya ultrasonik kaynaklı) ve kalıcı olmayan sistemler (ör. cıvatalı bağlantılar veya hücre yatağı ile mekanik olarak sabitlenmiş yapılar) olmak üzere iki gruba ayrılmıştır. Kalıcı olmayan düzenekler, ikinci yaşam uygulamaları için en uygun seçenek olarak belirlenmiş ve ikinci yaşam çerçevesinin temelini oluşturmuştur. Bu çerçeveyi desteklemek amacıyla, iki farklı SoH tahmin yöntemi geliştirilerek doğrulanmıştır. İlki, çevrim koşulları, şarj oranları ve DoD gibi etkenleri dikkate alan ayrıntılı bir model; ikincisi ise DCIR(%) değişimi ile çevrim sayısına odaklanan daha basit bir modeldir. Her iki model de güvenilir SoH tahminleri sunarak, kalıcı bağlantılar olmadan hücrelerin etkili bir şekilde ayrıştırılması ve yeniden kullanılması süreçlerini kolaylaştırmıştır. Ayrıntılı model, hücre yaşlanmasına dair daha fazla içgörü sağlarken; basit model, daha düşük test gereksinimleriyle pratik avantajlar sunarak ölçeklenebilir ikinci yaşam uygulamaları için uygun bir seçenek olmuştur. Bu modellerin farklı koşullarda doğrulanmasıyla, çalışma, invaziv olmayan tahmin araçları ve ölçeklenebilir çözümler sunarak batarya yeniden kullanımı için ikinci yaşam metodolojilerine katkıda bulunmaktadır.

Anahtar Kelimeler: Li-İyon, İkincil Ömür, SoH, Tahminleme-

ACKNOWLEDGEMENTS

I extend my gratitude to my employer, VESTEL, for providing the necessary resources and tools for this study, as well as supporting my pursuit of a master's degree alongside my professional responsibilities.

TABLE OF CONTENTS

LIST OF TABLES

LIST OF FIGURES

LIST OF ACRONYMS AND ABBREVIATIONS

Ah	Amphere - hour
ACIR	Alternative Current Internal Resistance
BPNN	Backpropagation Neural Network
BMS	Battery Management System
CC	Constant Current
CV	Constant Voltage
C-Rate	Current Rate
CIC	Cumulatively Integrated Current
DoD	Depth of Discharge
DDM	Data Driven Modelling
DCIR	Direct Current Internal Resistance
ECM	Equivalent Circuit Modelling
EIS	Electrochemical Impedance Spectroscopy
EVS	Electrochemical Voltage Spectroscopy
HI	Health Indicators
LiB	Lithium Ion Battery
LSTMNN	Long-Short-Term-Memory Neural Network
Li-Ion	Lithium Ion
LTO	Lithium-Titanite
MAPE	Mean Absolute Percentage Error

NC	Number of Cycles
NCM	Nickel-Cobalt-Manganese
RMSE	Root Mean Square Error
RFID	Radio Frequency Identification
RUL	Remaining Useful Life
SoC	State of Charge
SoH	State of Health
UI	User Interface
Wh	Watt - hour

1. INTRODUCTION

The invention of Lithium Ion Battery (LiB) has changed the dynamics and proficiency of portable electronics and energy storage systems. Currently, Lithium Ion (Li-Ion) cells are used in various applications like mobile phones, e-bikes, scooters, laptops, electric vehicles, etc. [1, 2]. Aside from consumer electronics, Li-Ion cells are also used to build batteries for smartcards, Radio Frequency Identification (RFID) tags, and biomedical sensors [3, 4, 5]. Currently, Li-Ion cells are the most popular energy storage choice because of their high energy density and power [6, 7]. Most of these electronic products would not be as efficient as now without Li-Ion. The main focus of this thesis is creating a non-invasive second-life framework and investigating the aging behaviors of these Li-Ion cells to be able to simulate and track the aging of cells.

Li-Ion cells have the ability to be able to hold energy within themselves and supply energy to devices whenever required. Li-Ion cells have high energy, low self-discharge ratings, higher safety levels and cycle life [8]. The ability to hold and release large amounts of energy when used in large groups is what enables applications like optimal renewable energy systems, electric vehicles, and hand-held mobile products. With the emergence of Li-Ion, energy-storing proficiency, and the flexibility of electronic devices, renewable energy technologies have improved on an immense scale. Li-Ion batteries, made from cells, reduce the wasted amount of generated renewable energies by storing overly generated energies and increase the use time of electronic devices such as mobile phones and mobile medical devices by being able to store a lot more energy compared with older energy storage technologies. The importance of Li-Ion technology not only comes from its ability to elevate energy storage technologies. Currently, energy demand is mostly supplied with fossil fuels, and with Li-Ion, humanity's dependency on fossil fuels will be reduced. Li-ion is one of the optimal solutions for replacing fossil fuels with green energy, which will lead to cleaner and more sustainable energy in the future. Despite

many of its highly beneficial properties, Li-Ion cells have their own downsides, starting from their lack of supply chain due to rare metals. These cells consist of rare metals with limited suppliers, mostly from African countries, such as lithium, nickel, manganese, and cobalt. These materials are expensive, limited, and hard to mine; therefore, they can be considered as not fully sustainable even though these materials are recycled from dead batteries. Aside from its supply chains, cells have a limited lifetime due to the deformation of materials inside these cells; therefore, they can not be used forever. When used for long periods, the energy and capacity of these cells fall off due to degradation, and when the degradation is at abnormal levels, it is possible to see safety accidents [9]. Lastly, Li-Ion cells have a failure mode called thermal runaway that may happen more likely with the aging, leading cells to overheat uncontrollably, leading to immense explosions. Since it is possible to observe safety risks over the usage time to ensure the safe and reliable operation of Li-Ion cells, there should also be techniques to estimate the health and degradation levels of these cells [10].

Cells and batteries are governed by a range of control parameters and performance indicators. Primarily, control involves monitoring charging and discharging current, along with discharging and charging voltage. These parameters describe the operational boundaries and technical constraints of cells and batteries. When assembling a battery or employing it for a final application, adherence to these boundaries is crucial. In terms of performance indicators, key parameters include Watt - hour (Wh), Amphere - hour (Ah), cycles, State of Charge (SoC), and SoH. The Wh signifies the power supply capacity of cells or batteries. It allows you to determine the duration over which a specific energy level can be supplied. To calculate the duration (T) equation (1.1) is used. The power capacity of cells P_{Cap} is divided by the intended rated power P_{Rated}.

$$T = \frac{P_{\text{Cap}}(Wh)}{P_{\text{Rated}}} \tag{1.1}$$

Cycles indicate the number of charge and discharge procedures applied to cells or batteries. Each full charge and discharge cycle represents one cycle. Cycles serve as one of the primary performance indicators commonly used to assess cell or battery aging. SoC indicates the ratio of remaining usable discharge capacity to maximum discharge capacity in the current health state. SoH, on the other hand, measures degradation in terms of discharge capacity compared to the rated capacity at manufacturing. As common acceptance, when SoH falls to ratios between 70-80%, cells and batteries are considered dead/retired batteries [11, 12, 13]. following definitions provide clarity: C_{Rated} represents the initial capacity of a newly manufactured cell, C denotes the remaining discharge capacity, and C_{Cmax} signifies the maximum deliverable discharge capacity at a given time, which can be calculated when the SoH is known. Definition of SoC can be seen in (1.2) while SoH can be seen in (1.3). Calculation of C_{Cmax} is also given in (1.4).

$$SoC = \frac{C}{C_{\text{Cmax}}} \tag{1.2}$$

$$SoH(\%) = \frac{C_{\text{Cmax}}}{C_{\text{Rated}}} * 100 \tag{1.3}$$

$$C_{\text{Cmax}} = C_{\text{Rated}} \times SoH \tag{1.4}$$

Li-Ion cells react in various ways in different applications, which affects SoH. Therefore, it is hard to estimate SoH of cells and batteries [14, 15, 16]. There are various estimation methods for SoH based on cells electrochemical models, equivalent circuit models, and data-driven models [17]. The electrochemical model consists of electrochemical processes occurring within cells. This model refers to mathematical expressions or simulations of these processes. The aim of this model is to explain ion and charge transfer, internal reactions happening within cells. This model's accuracy is significantly high

and can easily be adapted to different battery chemistry; however, it is very complex and requires large amounts of experimental data. Equivalent Circuit Modelling (ECM) represents the electrochemical processes with the battery with electrical circuitry using capacitors and resistors. ECM is simpler than electrochemical models, requiring less computational work, and is easier to use in battery applications; however, its simplicity leads to challenges when it is used for complex battery systems. Data Driven Modelling (DDM) on the other side do not work around chemical processes explicitly. Experimental data based on various properties of cells, such as temperature, current, and voltage, is used to train algorithms. DDM is much more suitable to real-world scenarios when their ability to handle large volumes of data is considered.

This thesis investigates the second-life framework potential of lithium-ion cells, emphasizing non-invasive approaches and state of health SoH modeling. The study begins with an analysis of the first life of batteries, covering manufacturing processes and the factors that determine their readiness for second-life applications. Battery assemblies are categorized into two groups: permanently connected systems, such as laser-welded or ultrasonically bonded, and non-permanent systems, such as bolted connections or mechanically secured cell beds. Non-permanent assemblies are identified as the most suitable for second-life applications, forming the foundation of a second-life framework.

To support this framework, efficient SoH estimation methods are developed and validated. Two models are proposed: a detailed model incorporating cycling conditions, charge rates, and depth of discharge DoD, and a simpler model focusing on changes in DCIR(%) value and cycle count. Both models demonstrate reliable SoH predictions, facilitating the effective sorting and reuse of cells without permanent interconnections. While the detailed model provides greater insights into cell aging, the simpler model offers practical advantages with lower testing requirements, making it suitable for scalable second-life applications. By validating these models under varied conditions, the study

contributes to second-life methodologies by presenting adaptable, non-invasive estimation tools and scalable solutions for battery reuse.

In addressing constraints commonly encountered by battery manufacturers—such as the need for cost-effective solutions and limited access to advanced hardware—this thesis underscores the importance of scalable, non-invasive estimation techniques. Experimental validation on commercial lithium-ion cells confirms the practicality of both models for real-world second-life scenarios. Furthermore, the significance of stable electrical connections is highlighted, as accurate DCIR measurements and consistent SoH estimates are crucial in the absence of permanent interconnections.

2. LITERATURE REVIEW

For the present study, a semi-empirical approach employing nonlinear regression has been adopted for model development. Although literature on such models has emerged over the past decade across various lithium-ion battery chemistries, it remains relatively underdeveloped. Numerous experimental inquiries have been undertaken to explore the impacts of diverse usage conditions.

In [18], the influence of accelerated life testing, with fluctuations in operating temperature, on LiFePO4/C lithium-ion batteries was explored. In paper, general stress factors of Li-Ion batteries in particular are given as elevated temperature, cycling at partial cycle depths, cycling at low and high SoC and high Current Rate (C-Rate). Effects of these stresses differ between different LiB chemistry. The influence of 5 common stress factors are proposed by scoring with a pentagon scale. Illustration of the effect of common stress factors can be seen in Figure 2.1.

Figure 2.1: *Common Stress Factors of LiB [18]*

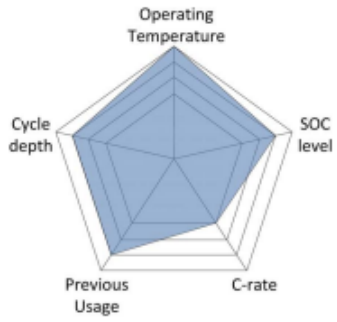

In paper, the stress factors have various nonlinear effects on the lifetime of the cells and in order to be able to observe real-life scenarios, testing methodologies need to consider at least three different stress factors. The selected stress factors include temperature, SoC, and cycle depth. Refer to Figure 2.2, based on SoC, cycle depth, and temperature, a 3-by-3 matrix is created to analyze the aging effect in the battery.

Figure 2.2: *Test Matrix of Study [18]*

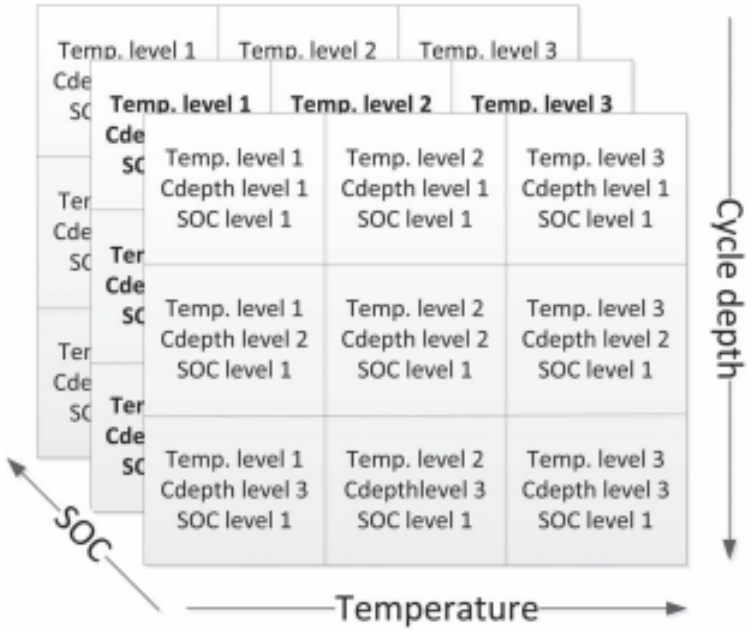

After the completion of these accelerated life tests, collected data has been analyzed and an equation for calculating the percentage rating of capacity fade in terms on completed Number of Cycles (NC) and temperature (T) as

$$C_{fade\_cyc}(NC, T) = 6.87 * 10^{-5} * \epsilon^{0.027*T} * NC^{0.5} \tag{2.1}$$

In paper[19], an empirical method is used for the estimation of SoH in terms of current rating, temperature, depth of charge. Study is done with two different cell models that has similar cathode-anode chemistry LiNiMnCoO2 graphite that has same level C-Rate only differing by capacity and their dimensions. Degradation of cells are investigated by evaluating the effects of :

- Constant Charging C-Rate
- Constant Discharging C-Rate
- High Temperature Operation

- Depth of Charge

- Dynamic Charging C-Rate

In study, two test matrices are used for the empirical data for 30 samples in total. 16 of samples which are cell type are given in Table 2.1 and Table 2.2.

Table 2.1: *Test Matrix For Cell A [19]*

Sr. No.	Charge C-Rate	Discharge C-Rate	Operating Temperature (°C)	Depth of Charge (%)	Dynamic Charge Profile	No. of replicates
1	2C	0.5C	25	100	N	2
2	1.5C	0.5C	25	100	N	2
3	1.5C	1C	25	100	N	1
4	1.75C	1C	25	100	N	2
5	1.5C	1C	25	75	N	2
6	1.5C	1C	25	50	N	2
7	1.5C	1C	40	100	N	1
8	2C	1C	25	100	Y	3
10	2.5C	1C	25	100	N	1
TOTAL						16

Table 2.2: *Test Matrix For Cell B [19]*

Sr. No.	Charge C-Rate	Discharge C-Rate	Operating Temperature (°C)	Depth of Charge (%)	Dynamic Charge Profile	No. of replicates
1	2C	0.5C	25	100	N	3
2	2C	1C	25	100	N	1
3	1.5C	1C	25	100	N	2
4	1.75C	1C	25	100	N	2
5	2C	1C	40	100	N	2
6	1.5C	1C	25	100	Y	4
TOTAL						

After completion of testing, non-linear regression is performed on test results. Equation (2.2) is built from the results of cell type A and equation (2.3) is generated from type B.

$$\mathrm{SOH} = 100 - 3.75\ \mathrm{N}^{0.47}\mathrm{C}^{2.17}\mathrm{e}^{-3932\left(\frac{1}{298}-\frac{1}{\mathrm{T}}\right)}\mathrm{IV}^{6.1} \tag{2.2}$$

$$\mathrm{SOH} = 100 - 6.1\ \mathrm{N}^{0.52}\mathrm{C}^{0.48}\mathrm{IV}^{1.75} \tag{2.3}$$

In paper [20] an advanced version of the model in [19] is used. To address the challenge of lithium-ion battery SoH estimation in real-world usage scenarios, a study into SoH degradation and developing a semi-empirical regression model for estimation is done. Initially, the model is trained using data from fixed cycling depths and charging currents, similar to typical laboratory conditions. To enhance the model's applicability to real-world scenarios, the study validated it by conducting tests with randomized cycling depths and current rating variations per cycle. Additionally, the study utilized various upper and lower SoC limits to simulate different user preferences. The test models were primarily categorized based on whether they used fixed or randomized parameters. The first test group, based on fixed-depth, involved testing cells with various combinations of different current ratings and operating temperatures. Test model of fixed depth program can be seen in Table 2.3.

Table 2.3: *Fixed-depth Test Models [20]*

$Use - parameter$	$Levels$
C-Rate	1.5C,1.75C,2C
Depth of Charge/ Discharge	50%, 75%, 100%
Operating Temperature	25°C, 40°C

Second test group has randomized depth and randomized current testing models. 4 different type of cycle randomization lower and upper bounds of SoC is applied. On the other hand, for randomization of c-rate they set current boundaries between 1-2.5C. Test table of randomized depth and current can be seen in Table 2.4.

In addition a study was also done for observing the effects of sampling time, test table study is as table 2.5.

Table 2.4: *Randomized Depth & Current Test Models [20]*

$TestType$	SOC $lower/upperbounds$	$C-rate$
Randomized Depth of Cycling	0 - 100% 60 - 100% 0 - 40% 30 - 70%	2C
Randomized C-Rate	0 - 100 %	1C - 2.5C
Combined Cycling	0 - 100% 60 - 100% 0 - 40% 30 - 70%	1.5C - 2C

Table 2.5: *Test Table [20]*

$Capacity$	$ModelTypes$	$Variants$	$Sub-Variants$
Conscious Agnostic	Exclusive Combined	1,2,3,4	Sampling Times(sec): 6,18,30,60,120,300,600,1200

In study, the models to adjust predictor variables to minimize their models estimation errors were repeated to improve the accuracy and robustness of SOH estimation. With the experimental data best fit to cell SoH is determined as Cumulatively Integrated Current (CIC) charging model. SoH model with the best fit is shared as equation (2.4) [20].

$$SOH = \; 0.53\,(\mathrm{SOH}_0)^{1.13}\, C^{-5E-3} \left(\frac{T}{298}\right)^{0.34} \left(\frac{V_{\text{avg,charge}}}{4.2}\right)^{-0.39} \left(e^{\frac{-29.34}{10^6} * \text{CIC}} + 0.03 e^{\frac{-7524.3}{10^6} * \text{CIC}}\right) \left(\frac{Cap}{100}\right)^{0.1} \tag{2.4}$$

In paper [21], a new methodology for estimating battery SoH by analyzing local voltage and capacity variations during charging/discharging is used. The paper reviews methods for estimating the SoH and predicting the Remaining Useful Life (RUL) of lithium-ion batteries, focusing on using local voltage and capacity variations during charging and discharging as key indicators. Method uses new SoH indexes, extracted from voltage and current profiles of an aging Nickel-Cobalt-Manganese (NCM)/ Lithium-Titanite (LTO) lithium-ion battery pack, and analyzes their relevance to battery capacity to derive a quantitative association model. The study further applies this model to estimate the SoH of a similar battery pack and predict its RUL using a particle filter algorithm. Study uses two types of SoH indexes: capacity variation at the same voltage interval and voltage variation at the same capacity interval. Each index type has two definitions, one for charging and one for discharging. The capacity variations during discharging and charging are represented by Q_{V-D} and Q_{V-C}, respectively, which are calculated as the integrals of the current and time between two voltage points. The voltage variations during discharging and charging are denoted as V_{Q-D} and V_{Q-C}, respectively, representing the voltage differences for the same capacity interval. To explain the acquisition of Q_{V-D}, study explained the calculation with the Figure 2.3. During discharging, two voltage levels is selected. While discharging with the constant current, study acquires the SoH index as product of time and current. The equation of the calculation is as shown in equation (2.5).

$$Q_{\mathrm{V-D}} = I \cdot (t_2 - t_1) \tag{2.5}$$

Figure 2.3: *Calculation of Q_{V-D}[21]*

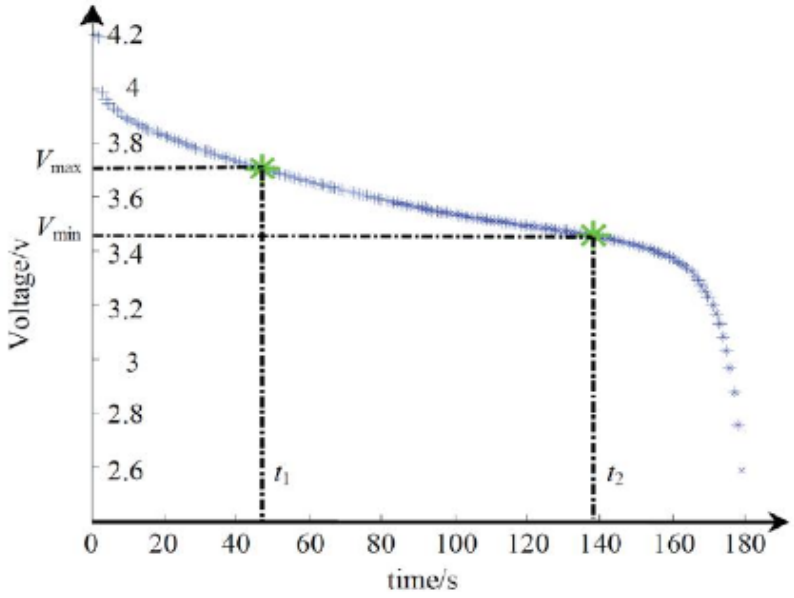

Study has 8 different SoH indexes with the data acquired from 100 cycles. Two two different approach for index generation, one is first order linear fitting and the other being second order quadratic fitting is used. According to results model can can estimate SoH with fitting errors less than %4 with all models. Study also highlights that the quadratic fitting has smaller errors. Equations and fitting errors of models are as in the Table 2.6.

Table 2.6: *Fitting Equation and error of SOH Indexes [21]*

$SOH Indexes$	$Linear Fitting$	$Errors$
$Q_{\mathrm{V-D}}$	$Q = 0.8418Q_{V-D} + 64.0124$	0.857
$Q_{\mathrm{V-C}}$	$Q = -30.0496Q_{V-C} + 114.9267$	1.1121
$V_{\mathrm{Q-D}}$	$Q = 1.0245V_{Q-D} + 65.7621$	0.8216
$V_{\mathrm{Q-C}}$	$Q = -21.2633V_{Q-C} + 113.1131$	0.7816
$SOH Indexes$	$Quadratic Fitting$	$Errors$
$Q_{\mathrm{V-D}}$	$Q = -0.0240Q_{V-D}^2 + 2.0053Q_{V-D} + 50.3549$	0.7954
$Q_{\mathrm{V-C}}$	$Q = -36.0476Q_{V-C}^2 + 41.8246Q_{V-C} + 79.5450$	0.9754
$V_{\mathrm{Q-D}}$	$Q = 0.0129V_{Q-D}^2 + 0.5955V_{Q-D} + 69.0271$	0.7618
$V_{\mathrm{Q-C}}$	$Q = -24.8214V_{Q-C}^2 + 44.3311V_{Q-C} + 70.4139$	0.4765

In paper [22], SoH estimation of used batteries are studied. In paper, estimation of SoH is done with analyzing the data gathered from retired batteries during their first life. Collected data from 12V 90Ah lead-acid batteries are analyzed with two different methods. Used analyze methods in paper are, Backpropagation Neural Network (BPNN) and Long-Short-Term-Memory Neural Network (LSTMNN). Study performed in paper can estimate the SoH of a retired lead-acid battery within 30 minutes while having a Root Mean Square Error (RMSE) less than %3. Estimation results are given in Figures 2.4 and 2.5 below.

Figure 2.4: *BPNN SoH Estimation[22]*

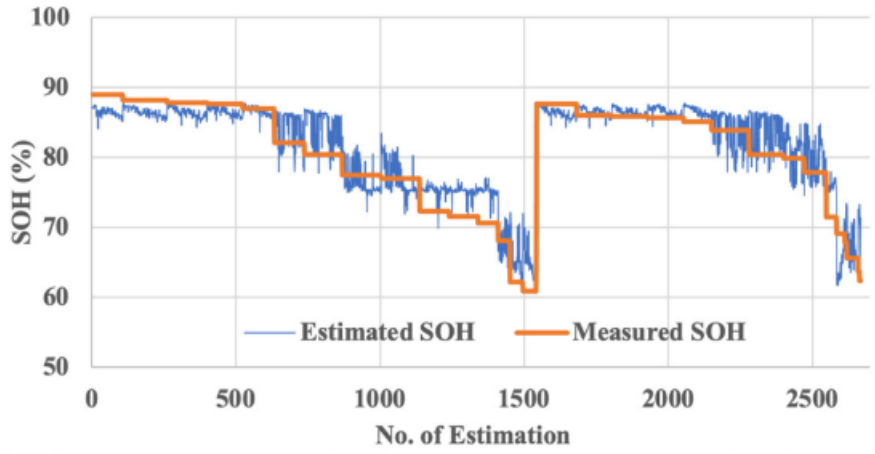

Figure 2.5: *LSTMNN SoH Estimation[22]*

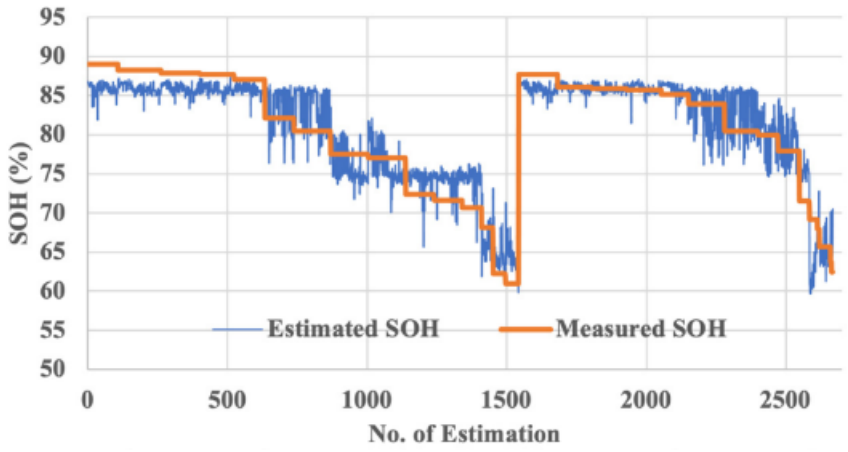

In paper [23] Electrochemical Impedance Spectroscopy (EIS) for SoH estimation on electrochemical electrodes is studied. In paper, a time-domain EIS measurement technique coupled with an interpretation utilizing equivalent circuit models is used. The precision of the measurements and the SoH estimation based on EIS are demonstrated through validation on Sanyo's UR14500P type LiCoO2 cells. Results indicate the efficacy of the proposed methods in swiftly and economically assessing LiBs.

In paper [24], methods for estimating the SoH of battery packs used in renewable

power plants and automotive applications are investigated. Various studies discuss various advanced techniques reported in the literature aimed at improving SoH accuracy for specific applications. However, implementing these methods practically is challenging due to complexities such as aging phenomena and operating conditions. This study proposes combining two basic estimation methods to create a real-time mixed algorithm, aiming for accurate SoH estimation while minimizing computational burden. Additionally, it integrates a prediction function to consider relaxation phenomena in no-load conditions. Experimental tests on batteries of different sizes and electrochemical technologies validate the proposed approach, demonstrating its accuracy compared to other common SoH estimation methods.

In paper [13] cycling performance and aging mechanisms of Li-Ion pouch batteries are studied. Li-Ion cells are cycled under various charging & discharging currents, DoD and temperatures. Empirical data generated from the test cells are analyzed with Electrochemical Voltage Spectroscopy (EVS). In study, to make EVS work with high current ratings, electromotive-force extraction method is adapted. Study established multiple linear regression algorithms that can estimate the SoH of batteries under 3% absolute error.

In paper [12] a SoH estimation based on Health Indicators (HI) which are derived from discharge characteristics of Li-Ion batteries are used. Voltage drop observed during discharging and the time needed to observe same voltage difference during discharging are accepted as the indirect HI of the capacity estimation. An optimal discharge voltage is selected with a genetic algorithm which was also verified. Generated degradation model is used to trained LSTMNN. Used method can predict with a Mean Absolute Percentage Error (MAPE) under 0.41% averagely.

3. METHODOLOGY

In this chapter, the first and second life cycles of cells and batteries are initially discussed. Following this, the design phase of the thesis is explained in detail, highlighting the core components of the study and their interconnections. Key elements such as the test plan, sample organization and the test devices used in the research are described in detail. Additionally, the processes involving test setups, sample selection methods, sample grouping strategies, and data handling are outlined in the following sections.

3.1 Cell and Battery Life Cycle

In this thesis, the development of an optimal estimation model for SoH of cells in second-life applications is studied. To understand this work, it is important to first explain the life cycle of cells and batteries. While general terminologies are commonly accepted, explaining key aspects of battery and cell life is necessary to assess the applicability of this study. The following sections will explain the concepts of primary and secondary life cycles.

3.1.1 First Life of Cells and Batteries

Figure 3.1: *First Life Cycle of Cells and Batteries*

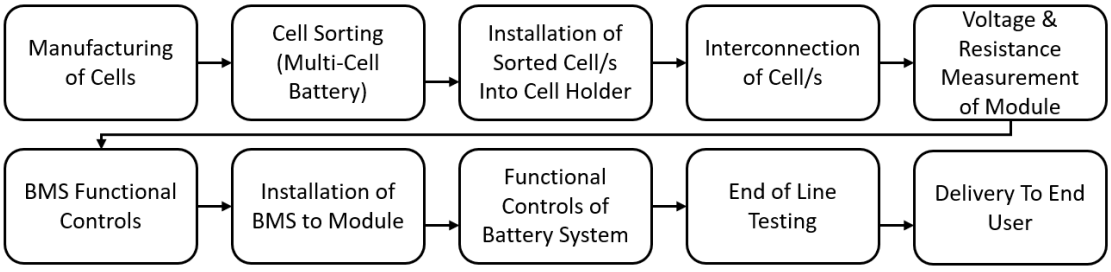

As illustrated in Figure 3.1, the first life of cells and batteries (a battery being a single cell with a Battery Management System (BMS) is also a battery) begins with the manufacturing of cells. Cell manufacturers deliver cells with a 30% SoC to battery

manufacturers, as required by United Nations shipping regulations. Even though these cells share the same SoC, they differ in voltage and internal resistance, which becomes critical for the cell balancing process, especially in batteries with parallel-connected cell blocks.

The next step in the process is cell balancing, which equalizes the voltage of the cells in a battery, as mandated by safety standards. Beyond regulation, cell balancing ensures that the cells operate efficiently. After completing this balancing process, the cells are grouped and placed in fixtures (cell holders), where their interconnections are made. The type of interconnections varies depending on the cell type and the application. For example, pouch cells may have their terminals soldered or clamped, while prismatic cells with bolt nests can be interconnected using bolts.

Once the interconnections are completed, the assembled battery module undergoes quality control. In this step, the internal cell connections are verified by measuring the voltages of the cells and module terminals. Additionally, the resistance of the module is checked to ensure it meets design limits and minimizes conduction losses.

Following this, attention shifts to the BMS, which is tested before installation to ensure it can accurately measure temperature, voltage, and current, and that its protection functions are operational. After the standalone BMS passes its functional tests, it is installed in the battery module, and the full battery system undergoes similar tests to verify its functionality.

Finally, after confirming that the battery system functions correctly, the entire module is subjected to a stress test involving several cycles. This guarantees that the battery operates as intended under load. Once this aging process is complete, the batteries are prepared for shipment to the end user, marking the starting point of the first life.

3.1.2 Second Life Life of Cells and Batteries

The second life of a cell or battery begins after its first life ends. The end of the first life is subjective, depending on both the user and the battery designer. Generally, a cell or battery is considered to have reached the end of its first life when its SoH drops to 80%. At this point, it is seen as having fulfilled its expected lifetime. Several studies explore the usability of cells or batteries after they reach 80% SoH. However, since this limit is subjective, some cells and batteries may lose their primary purpose before reaching 80%.

Given the effort required to scrap or recycle these cells and batteries, re-purposing them for different applications becomes an alternative approach. The first important step in second-life applications is to assign an accurate SoH to the batteries or the individual cells used in battery assemblies. While measuring the SoH of small numbers of products may not pose a significant challenge, when second-life applications involve large quantities, measuring each one individually is not feasible due to the time required. To make second-life applications scalable, a reliable and efficient method for tracking the SoH of these products is essential. Although there are several methods for estimating the SoH of a battery or cell, many require active measurements during usage, which is not practical when dealing with large quantities.

With this in mind, second-life applications can be approached at both the cell level and the battery level. However, re-purposing individual cells disassembled from batteries presents greater challenges due to variations in degradation across cells. Managing the second life of whole battery assemblies is more straightforward, especially when the system has only lost efficiency in its first-life application. In such cases, the primary difficulty is disconnecting the battery system from its original application.

For mobile applications, designers often use permanent connection methods, such as laser or ultrasonic welding, to secure cells in place as given in Figure 3.2.

Figure 3.2: *Permanent Interconnection of an E-Bike Battery*

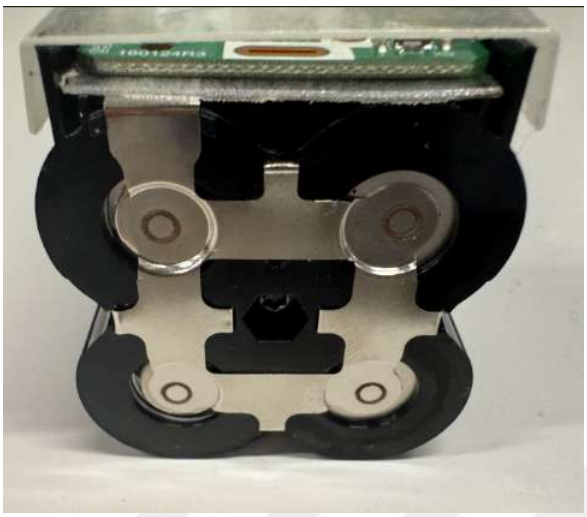

While these methods improve durability, they make disassembly for second-life use more complicated. For battery systems with non-permanent connections, the process of disassembly and inspection is simpler.

Figure 3.3: *Second Life Cycle of Batteries with Permanent Interconnection*

During inspections, not only is SoH assessed, but the condition of components like interconnects, wiring, and metal parts is also evaluated to ensure they function at an acceptable level. Batteries that meet these standards can be repurposed for other devices, especially for less demanding applications, where lower energy or power performance is still suitable. Optional scenario for second-life applications, particularly for batteries that has permanent connections between cells, is illustrated in Figure 3.3.

Second life on cell level has its own challenges starting with the acquiring of the cells. These cells can be either collected by disassembling multi-cell modules/batteries or can be acquired from small devices that either only uses cell like remote controllers or from single-cell batteries such as mobile phones. Hardest option would be again disassembling cells from the batteries, especially if the battery has permanent interconnections where disassembly must not damage the cells. Example prismatic bolted cell for batteries that are usable for non-permanent connection batteries is shown in Figure 3.4.

Figure 3.4: *Bolted Prismatic Batteries without Permanent Interconnection*

Both type of cell second life methods have similarities in their second life processes. However, as mentioned in previous paragraph acquiring cells from the battery assemblies is harder.

As illustrated in Figure 3.5, initial step is the gathering of batteries that are deemed as full-filled their first life which also includes the SoH level of cells/modules inside of it. After the initial gathering, the batteries are sorted similar to cells being sorted at the

Figure 3.5: *Second Life Cycle of Batteries without Permanent Interconnection*

start of battery manufacturing. This enables to collect cells that almost have identical parameters. Which kinda means that they are the lesser versions of themselves when compared to fresh manufactured cells. In this scenario, if the disassembly of cells actually does not pose a challenge when the battery does not assemble with permanent connection methods. Initially batteries that are ready for second life are collected from end users. Initial process is the sorting/grouping the batteries that are in the same SoH region. With the completion of battery sorting according to SoH, next step is the controlling mechanical integrity of battery to observe that if there are any mechanical failures on cells. Normally damaged cell in a fully functional battery is not accepted however with the multi-cell battery assemblies there may be scenarios that due to large tolerances set in BMS, it is possible to have couple cell blocks having a disconnected cell or cells. However, this is an uncommon failure mode that will most likely for only batteries that assembles from cells block that have huge amount of cells connected in parallel. In this type of an battery depending on the amount of parallel connected cells, losing one cell may not alert the end user with a permanent shutdown failure. Therefore, it is important to control the mechanical components of battery after sorting them. With the completion of inspection of the battery mechanical components, cells are uninstalled from the battery to start the manufacturing of either new battery or installed in the new equipment for the products that only require cell/s.

Alternatively for second life also cells can be standalone acquired from the end user products such as remote controllers, mobile phones, medical devices that do not

have permanent connection method. This type of cells that are used in single cell or serial connected non parallel connected batteries are common in the current market to be able to make frequently used rechargeable consumer electronics. These type of applications generally have general typical usage scenarios in stabilized environments. These types of products generally have a highly estimable life cycles therefore, they are considered as the most optimal type of cells/batteries to initiate second life applications.

As explained in Figure 3.6, after the gathering of cells, cells are sorted based on their SoH and put under mechanical inspection to control that cells did not go under mechanical degradation. With clarification of cells that they only lost their capacity, they can be deemed suitable for secondary life use.

Figure 3.6: *Second Life Cycle of Cells without Permanent Interconnection*

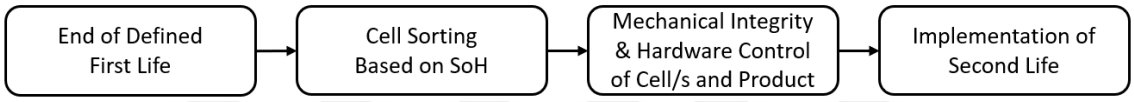

3.2 Integration of SoH Estimation to Battery First and Second Life

This section explains how the developed SoH estimation models can be integrated into both first-life and second-life battery applications. The discussion focuses on practical implementation steps for each model, emphasizing how they leverage cell behavior under various parameters and conditions. Because each model is designed to address different usage scenarios, their respective application procedures differ accordingly.

As noted in Section 3.1, second-life and SoH estimation methods are primarily intended for single-cell or multi-cell configurations lacking permanent interconnections. This design choice supports flexible reconfiguration and scalable deployment, making the models particularly suitable for second-life scenarios where cost effectiveness and ease of assembly are critical. The following subsections outline the key considerations for

implementing each model and detail the necessary data collection and analysis procedures for effective SoH estimation in both first and second life contexts

3.2.1 Implementation of Detailed Model

The detailed model requires aging data input, consisting of cycle count, charge current rating, and depth of discharge DoD. To implement this model, battery manufacturers must first develop an aging test plan that accounts for both first-life and second-life applications. The accuracy of the model improves as the variety of key parameters increases. Therefore, manufacturers should conduct multiple aging tests that include various charge current rates and DoD levels. These primary parameters must be defined for cycling with a target number of cycles, ensuring that the test plan covers a representative range of operating conditions.

Since SoH estimation and its interpretation require a consistent reference point, manufacturers must establish a standardized SoH measurement procedure, including a uniform charging and discharging profile. Cell manufacturers typically provide general life cycle aging data in their technical specifications, which often use a 0.2C discharge rate and a charging method that aligns with design limitations. Using this reference, the measurement profile for SoH should be finalized to maintain consistency across tests.

Once the measurement profile is established, cells must be cycled according to the predefined aging profiles. At regular intervals after a specified number of cycles, cells or battery packs should undergo a full SoH assessment using the standardized profile. This structured process results in a dataset that maps SoH evolution as a function of cycle count, charge rate, and DoD. By following this schedule, manufacturers can generate a comprehensive data pool that captures SoH behavior across different aging scenarios. This data pool is then used to develop a detailed estimation model similar to the one designed in this study.

Once sufficient aging curves are collected, the model constructs an estimated SoH per cycle curve, predicting how SoH changes over time under different conditions. This process continues until the expected end-of-life threshold of the battery is reached, at which point the full SoH trajectory for the battery's first life is established. The next step is determining the SoH threshold that marks the transition from first-life to second-life usage. As discussed earlier, this threshold varies depending on the requirements of the application. Once a battery reaches its designated first-life SoH limit, it is collected from customers. At this stage, the battery in the customer's product is replaced, while the retrieved battery undergoes an inspection process to assess its suitability for second-life applications, following the procedure outlined in Figure 3.6.

Throughout the battery's first life, the estimation model utilizes data acquired from BMS to monitor degradation. By the time the battery enters second-life consideration, its SoH is already known. With this information, manufacturers can determine the new starting cycle count for the battery's second life application. Additionally, by analyzing the aging curves and cycle dependencies established during first-life testing, manufacturers can estimate how many additional cycles the battery can sustain in its second-life role, effectively determining its Remaining Useful Life (RUL).

3.2.2 Implementation of Simpler Model

The simpler SoH model requires aging data input, consisting of cycle count and % changes in direct current internal resistance DCIR. To implement this model, battery manufacturers must first develop an aging test plan that tracks DCIR evolution throughout the battery's intended first-life operation. Since this model does not rely on charge current or DoD variations, it requires fewer test parameters but still demands structured aging data to ensure accurate predictions.

Since SoH estimation is based on DCIR progression, manufacturers must establish

a standardized measurement process. The initial DCIR value is recorded at the beginning of the battery's life to serve as a baseline. As the battery undergoes cycling, DCIR measurements are collected at predefined intervals. These measurements can be obtained either through controlled aging tests or real-world operational data from the battery management system BMS. To ensure reliability, measurements should be taken under stable conditions to minimize the influence of external factors such as temperature fluctuations, inconsistent fixation of cells or transient load changes.

Once the measurement protocol is established, cells must be cycled according to a predefined aging schedule. After a specified number of cycles, DCIR is reassessed to monitor resistance increase over time. This structured process generates a dataset that correlates DCIR changes with cycle count, allowing the development of an estimation model similar to the one designed in this study. By analyzing this dataset, manufacturers can determine expected SoH values at various stages of battery aging.

As the aging process continues, the model constructs an estimated SoH per cycle curve based on DCIR changes. This curve enables manufacturers to predict the expected end of life thresholds for first-life applications. Since the transition from first-life to second-life usage depends on application requirements, manufacturers must define the appropriate SoH threshold. Once a battery reaches this limit, it is collected from customers and evaluated for second-life suitability, following the procedure outlined in Figure 3.6.

Throughout the battery's first life, BMS data allow continuous monitoring of degradation. By the time the battery is considered for second-life applications, its SoH is already known, enabling manufacturers to determine a new starting cycle count for second-life usage. By referencing historical DCIR progression, the model estimates how many additional cycles the battery can sustain under second-life conditions, effectively determining its remaining useful life RUL. This structured approach provides a cost-effective and scalable method for evaluating battery aging and optimizing second-life

applications with minimal additional testing.

3.3 Research Design

This thesis undertakes a detailed examination of cell aging processes, which are critical for understanding the degradation mechanisms of Li-Ion cells to find an optimal estimation for the second life of cells. The research design includes three distinct phases, each aimed at addressing specific aspects of cell aging dynamics within a formal framework. Initially, the research focuses on detailed modeling, where numerous parameters that control cell performance are analyzed. Variables such as SoH, charge rate, and cycling frequency undergo thorough inspection with the goal of constructing a predictive model that can distinguish interactions between these factors and the aging trajectory of cells. Through systematic experimentation and data generation, the objective is to achieve a comprehensive understanding of cell performance under various operational conditions. Following this, the research transitions to the critical phase of model validation, which requires verification of the predictive framework developed against empirical data. A diverse array of testing cells that represent different operating scenarios is arranged, allowing for an estimation of the model's impact. By subjecting the model to real-world conditions and comparing its predictions against observed outcomes, this phase aims to validate the model's accuracy and predictive capability, thereby enhancing its applicability and reliability in practical settings for the second life of cells. Finally, the investigation explores alternative methodologies for estimating aging, diverging from conventional modeling paradigms. By focusing on fundamental indicators such as cycle count and DCIR variations (%), a new estimation methodology is proposed, offering an effective approach to predicting cell aging. Through experimentation and validation processes, the viability and accuracy of this alternative approach are examined, aiming to enrich the aging prediction techniques available to researchers and industry stakeholders

for second-life applications.

In summary, this research design embodies a structured effort to find optimal methods of SoH estimation through cell aging. By integrating detailed modeling, validation, and the exploration of alternative estimation methods, the research aims to realize and validate effective estimation techniques. Based on the results, the accuracy and practicality of these models will be evaluated for second-life applications of cells.

3.4 Data Collection and Equipment

To manage the charge and discharge cycles of cells, precise control of both current and voltage is essential. The procedure begins with discharging the cells at a constant current until the minimum discharge voltage is reached, followed by a rest period. Subsequently, the cells are charged with a constant current until the maximum charging voltage is achieved. The charging then transitions to a constant voltage mode until the current decreases to the level specified by the manufacturer. After the charging process has been completed, the cells are discharged to the desired current level and minimum discharge voltage. The capacity is determined by integrating the current-time graph, which calculates the capacity in Ah at the specified discharge current level, along with other pertinent parameters.

To enable an accurate prediction of the SoH in this study, it is crucial to develop or acquire an intelligent cell simulator. This system must provide continuous monitoring and control of the cell, utilizing current and voltage sensors to capture real-time data. It should also incorporate temperature sensors to monitor and regulate both environmental and cell surface temperatures. The simulator must be capable of calculating cell capacity independently at the end of both discharge and charge cycles using the Coulomb counting method. A schematic representation of the proposed system is provided in Figure 3.7.

Figure 3.7: *Block Diagram of the Testing Procedure*

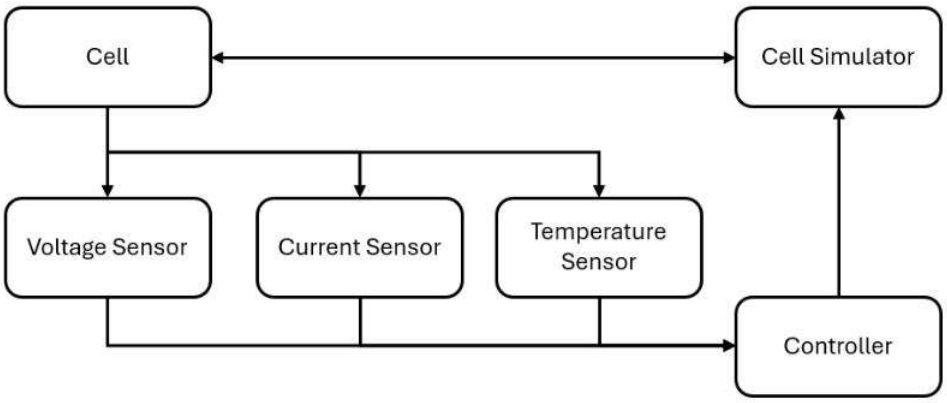

Testing setup used in this research work is shown in Figure 3.8, whereas the test bench is shown in Figure 3.9. The charge/discharge, or cycling processes necessary for this study, along with the measurement of ambient temperature, were conducted using a calibrated cell simulator. During testing, parameters such as current, voltage, temperature, cycle count, etc., read by sensors, were recorded by this simulator. Electrical connections required for charge and discharge processes were provided with special cell fixtures produced for cycle tests.

Figure 3.8: *Experimental Setup for Testing Li-ion Battery Cells*

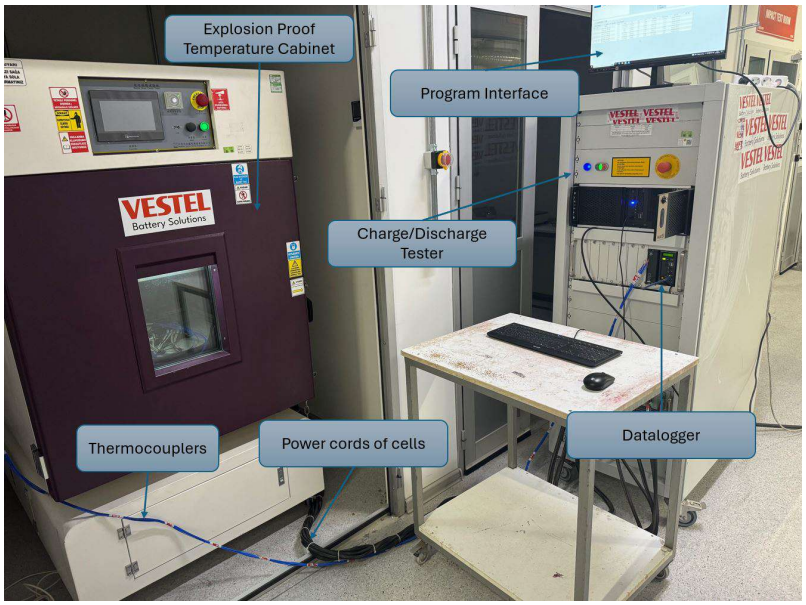

Figure 3.9: *Li-ion Battery Cells Undergoing Evaluation in the Testing Chamber*

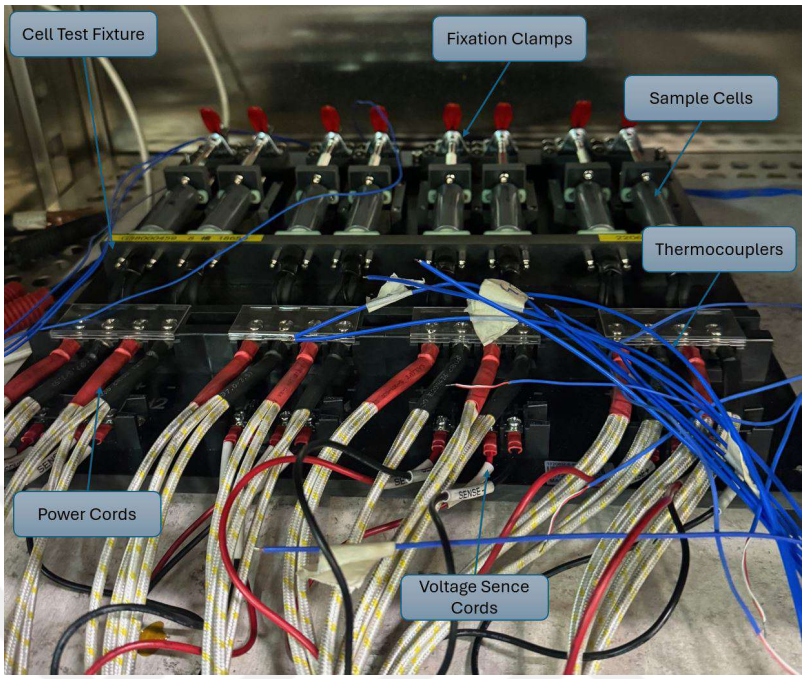

3.5 Sampling Strategy

This study focuses on commercially available lithium-ion cells, emphasizing a technical investigation into the impacts of charging current, cycle number, DoD and change of DCIR. The primary characteristics of the cells under test are summarized in Table 3.1. Our primary aim is to develop a robust estimation model capable of predicting the SoH of cells sharing the same model characteristics. Through empirical analysis and mathematical modeling, we derive methods that can accurately estimate the SoH of products assembled from these commercialized cells. This model will serve as a tool in assessing battery health, optimizing product performance, and facilitating informed decision-making regarding warranty determination and quality assurance processes. To align with the aim and scope of this paper, we have selected commercially available cells from a prominent industry manufacturer.

Table 3.1: *Properties of Device Under Test*

$Parameters$	$Value$
Energy	17.7 Wh
Capacity	4800 mAh
Nominal Voltage	3.69 V
Operation Voltages	2.5 - 4.2 V
Std. Charge	0.3C Constant Current (CC) 4.2 V Constant Voltage (CV) Cut off at 50 mA
Std. Discharge	0.2C Discharge Cut off at 2.5 V
Max Charge Current	0.7C
Max Discharge Current	1.5C at 25-55 Celcius

Four sample groups were organized to study lithium-ion battery degradation. The first group of samples G1, is arranged to collect data by using various charge currents,DoD, and cycling frequencies to understand their effects on battery health. The second group of samples G2, is arranged to validate estimation model which is generated by training regression learner in MATLAB with the collected data from the cells of G1. The third group of samples G3, focuses on observing degradation in terms of cycle count and changes in DCIR, provided additional data for model development. Finally, the fourth group OF samples G4, is arranged to validate estimation model which generated from the cell data of G3. This structured approach, detailed in Table 3.2, helps build a two different estimation models.

Table 3.2: *Illustration of Sample Groups*

Group No.	*Sample ID*	*Aging Model*	*Cycle*	*Chg. Curr*	*Disch. Curr.*	*DoD (%)*
G1	004	Model 1	300	0.4C	1C	50
	005	Model 1	300	0.4C	1C	50
	008	Model 2	450	0.5C	1C	60
	010	Model 2	450	0.5C	1C	60
	019	Model 3	500	0.6C	1C	70
	028	Model 3	500	0.6C	1C	70
	029	Model 4	600	0.7C	1C	80
	030	Model 4	600	0.7C	1C	80
G2	003	Model 5	300	0.7C	1C	100
	009	Model 6	450	0.7C	1C	80
	011	Model 7	500	0.7C	1C	60
	012	Model 8	600	0.7C	1C	40
G3	001	Model 9	300	0.7C	1C	100
	002	Model 10	450	0.7C	1C	100
	006	Model 11	500	0.7C	1C	100
	007	Model 12	600	0.7C	1C	100
G4	021	Model 13	300	0.7C	1C	100
	014	Model 14	450	0.7C	1C	100
	017	Model 15	500	0.7C	1C	100
	023	Model 16	600	0.7C	1C	100

3.5.1 Organization of Sample Groups

As indicated in Table 3.2, the study employs multiple test profiles to develop two different estimation methods. Sample Group G1 forms the basis for a detailed estimation model that incorporates cycle count, charging current, and depth of discharge. On the other hand, a simpler estimation model uses cycle count and changes in DCIR as input parameters. Analysis of the core parameters come up to a conclusion that the detailed model requires cells with similar Alternative Current Internal Resistance (ACIR) to enhance accuracy. In contrast, the simpler model, which relies on changes in DCIR, requires sample groups with different ACIR levels to ensure a diverse resistance range among the

cells. Initially, 30 commercial cells are acquired for the study, and their zero-hour voltages and ACIR are measured for selection. These measurements are detailed in Table 3.3. To measure ACIR, calibrated battery and cell internal resistance measurement which is shown in Figure 3.10.

Table 3.3: *Sample Distiribution and Measured Values*

Sample Name	Zero Hour IR AC	Zero Hour IR DC	Voltage	Group
2024-01-001	14.10	14.25	3.568	Res Based Est.
2024-01-002	14.25	14.25	3.567	Res Based Est.
2024-01-003	14.25	14.20	3.569	Validation Tests
2024-01-004	14.20	14.20	3.571	In-Depth Est.
2024-01-005	14.20	14.30	3.569	In-Depth Est.
2024-01-006	14.50	14.20	3.568	Res Based Est.
2024-01-007	14.37	14.20	3.569	Res Based Est.
2024-01-008	14.20	14.30	3.569	In-Depth Est.
2024-01-009	14.60	14.60	3.565	Validation Tests
2024-01-010	14.22	14.22	3.568	In-Depth Est.
2024-01-011	14.31	14.10	3.568	Validation Tests
2024-01-012	14.10	14.01	3.564	Validation Tests
2024-01-013	14.01	14.01	3.564	Validation Tests
2024-01-014	14.75	14.10	3.565	Res Based Est.
2024-01-015	14.10	14.00	3.569	Validation Tests
2024-01-016	14.00	14.30	3.566	Res Based Est.
2024-01-017	14.30	14.10	3.569	Res Based Est.
2024-01-018	14.10	14.10	3.568	Validation Tests
2024-01-019	14.20	14.13	3.567	In-Depth Est.
2024-01-020	14.13	14.00	3.565	-
2024-01-021	14.00	14.30	3.566	Res Based Est.
2024-01-022	14.30	14.35	3.568	Validation Tests
2024-01-023	14.35	14.10	3.567	-
2024-01-024	14.35	14.10	3.568	In-Depth Est.
2024-01-025	14.10	14.10	3.572	-
2024-01-026	14.10	14.00	3.570	-
2024-01-027	14.00	14.25	3.569	In-Depth Est.
2024-01-028	14.25	14.20	3.568	In-Depth Est.
2024-01-029	14.20	14.05	3.567	In-Depth Est.
2024-01-030	14.20	14.20	3.568	In-Depth Est.

Figure 3.10: *Battery and Cell Internal Resistance Tester*

3.5.2 Test Plan

For the generation of estimation models, ensuring reliability requires testing at multiple levels. Cells selected for each group must align with the fundamental requirements of the chosen method. While testing at different levels provides the benefit of covering a broad range of conditions, it also complicates SoH measurement, especially when models involve varying DoD. Therefore, SoH needs to be measured after each checkpoint during the testing phase to allow the algorithm to better account for the effects of key parameters.

As shown in Figure 3.11, the test plan begins with cell sorting to select the most suitable cells for the respective test groups. The selected cells are cycled using the manufacturer's standard charge and discharge profile to determine the zero-hour capacity, which will be used to calculate SoH. Additionally, cells in groups G3 and G4 undergo DCIR measurement. After the zero-hour measurements, the cells are ready to be cycled with the profiles assigned to them, as outlined in Table 3.2. Each cell undergoes ten aging

Figure 3.11: *Test Plan of Aging*

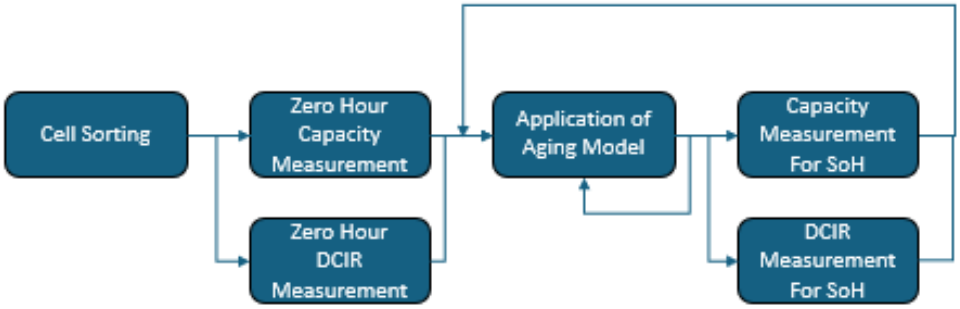

cycles, followed by cycling with the manufacturer's standard cycle to measure capacity for SoH calculation. Cells in G3 and G4 also undergo DCIR measurement to track this key parameter for the second estimation model. This process is repeated after each set of measurements until the target cycles are reached.

3.5.3 Calculation of DCIR

$$DCIR = \frac{V_1 - V_2}{I_2 - I_1} \tag{3.1}$$

The DCIR of batteries and cells can be measured using several methods. The most commonly accepted method, as per LiB standards, involves measuring the voltage changes under varying loads, described in (3.1). Firstly, the battery is discharged at a rate of 0.2C, defined as I_1, for 10 seconds to record the voltage V_1. Following the 10 second discharge, a discharge rate of 1C is applied for 1 second noted as I_2 to measure the final voltage V_2. The DCIR is then calculated by dividing the voltage difference ($V_1 - V_2$) by the current difference ($I_2 - I_1$).

3.6 Generation and Usage of Data

This thesis focuses on the aging data of commercialized Li-ion cells. Since such data is crucial for the analysis, it must either be acquired directly from the manufacturer or generated independently for the purpose of the study. Manufacturer-supplied data, however, is often limited and may not always reflect the exact performance characteristics, leading to potential inaccuracies. To ensure an objective and reliable approach, all the data used in this study was generated in-house. As described in the ”Data Collection and Equipment” section, a unique cell tester was employed to cycle the test samples and collect data continuously throughout the testing process. Upon completing the test program, a comprehensive Excel report was generated, containing vital information such as voltage, current, cycles, capacity, energy, power, and measured temperature for each cell. For the more detailed model created from the G1 data, cycle count, charge current, and depth of discharge were used as input variables. In contrast, for the simpler method based on the G3 data, cycle count and the percentage change in DCIR were the primary input parameters.

A sample of the raw data output acquired from the cell tester is shown in Figure 3.12. This figure illustrates the structure and key parameters included in the dataset, providing an overview of the variables tracked throughout the cycling process.

Figure 3.12: *Example Output From Cell Tester*

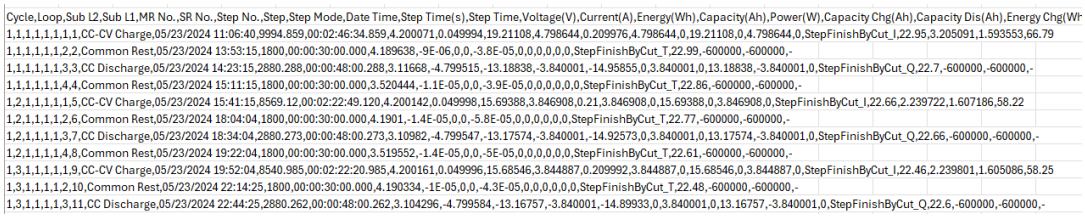

```
Cycle,Loop,Sub L2,Sub L1,MR No.,SR No.,Step No.,Step,Step Mode,Date Time,Step Time(s),Step Time,Voltage(V),Current(A),Energy(Wh),Capacity(Ah),Power(W),Capacity Chg(Ah),Capacity Dis(Ah),Energy Chg(Wh
1,1,1,1,1,1,1,1,CC-CV Charge,05/23/2024 11:06:40,9994.859,00:02:46:34.859,4.200071,0.049994,19.21108,4.798644,0.209976,4.798644,0,19.21108,0,4.798644,0,StepFinishByCut_I,22.95,3.205091,1.593553,66.79
1,1,1,1,1,1,2,2,Common Rest,05/23/2024 13:53:15,1800,00:00:30:00.000,4.189638,-9E-06,0,0,-3.8E-05,0,0,0,0,0,0,StepFinishByCut_T,22.99,-600000,-600000,-
1,1,1,1,1,1,3,3,CC Discharge,05/23/2024 14:23:15,2880.288,00:00:48:00.288,3.11668,-4.799515,-13.18838,-3.840001,-14.95855,0,3.840001,0,13.18838,-3.840001,0,StepFinishByCut_Q,22.7,-600000,-600000,-
1,1,1,1,1,1,4,4,Common Rest,05/23/2024 15:11:15,1800,00:00:30:00.000,3.520444,-1.1E-05,0,0,-3.9E-05,0,0,0,0,0,0,StepFinishByCut_T,22.86,-600000,-600000,-
1,2,1,1,1,1,1,5,CC-CV Charge,05/23/2024 15:41:15,8569.12,00:02:22:49.120,4.200142,0.049998,15.69388,3.846908,0.21,3.846908,0,15.69388,0,3.846908,0,StepFinishByCut_I,22.66,2.239722,1.607186,58.22
1,2,1,1,1,1,2,6,Common Rest,05/23/2024 18:04:04,1800,00:00:30:00.000,4.1901,-1.4E-05,0,0,-5.8E-05,0,0,0,0,0,0,StepFinishByCut_T,22.77,-600000,-600000,-
1,2,1,1,1,1,3,7,CC Discharge,05/23/2024 18:34:04,2880.273,00:00:48:00.273,3.10982,-4.799547,-13.17574,-3.840001,-14.92573,0,3.840001,0,13.17574,-3.840001,0,StepFinishByCut_Q,22.66,-600000,-600000,-
1,2,1,1,1,1,4,8,Common Rest,05/23/2024 19:22:04,1800,00:00:30:00.000,3.519552,-1.4E-05,0,0,-5E-05,0,0,0,0,0,0,StepFinishByCut_T,22.61,-600000,-600000,-
1,3,1,1,1,1,1,9,CC-CV Charge,05/23/2024 19:52:04,8540.985,00:02:22:20.985,4.200161,0.049996,15.68546,3.844887,0.209992,3.844887,0,15.68546,0,3.844887,0,StepFinishByCut_I,22.46,2.239801,1.605086,58.25
1,3,1,1,1,1,2,10,Common Rest,05/23/2024 22:14:25,1800,00:00:30:00.000,4.190334,-1E-05,0,0,-4.3E-05,0,0,0,0,0,0,StepFinishByCut_T,22.48,-600000,-600000,-
1,3,1,1,1,1,3,11,CC Discharge,05/23/2024 22:44:25,2880.262,00:00:48:00.262,3.104296,-4.799584,-13.16757,-3.840001,-14.89933,0,3.840001,0,13.16757,-3.840001,0,StepFinishByCut_Q,22.6,-600000,-600000,-
```

With this dataset in hand, additional spreadsheets were created to facilitate the training of regression models. These spreadsheets included key parameters such as cycle count, charge current, DoD, capacity, and SoH. This organized data allowed for a more

effective model training process, where detailed patterns could be extracted to support the estimation model development.Once the spreadsheets were generated for the cells in groups G1 and G3, they were utilized to train several regression models implemented in MATLAB. The objective was to determine the most accurate estimation models for the respective data sets. In MATLAB, these regression models use the provided data as inputs to establish a correlation between the input parameters and the output parameter, SoH. A visual summary of these trained models, including their performance metrics, is shown in User Interface (UI) Figure 3.13. This figure provides a comparative view of the various models trained using different combinations of input variables, allowing for a comprehensive evaluation of their accuracy and predictive capabilities.

Figure 3.13: *Part of UI From Regression Learner*

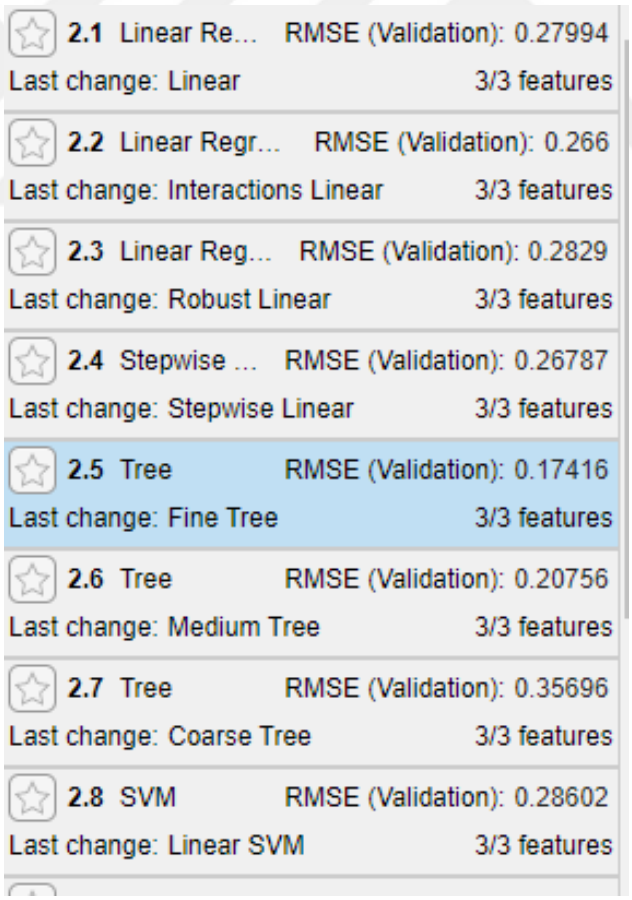

4. RESULTS

In this section, the test results of the sample groups are presented and analyzed. Sample groups G1 and G3 are utilized to generate data for the estimation models, with a focus on comparing and analyzing the fit between the estimated and measured SoH values. Sample groups G2 and G4 are used for validating the estimation models. Accordingly, the following sections compare the estimation curves with the measured SoH curves and provide the RMSE values for each group. All results are evaluated and discussed in detail in Section 5, ”Discussion.”

4.1 Sample Group G1

In, Figure 4.1, aging curves of the cells are illustrated and as explained in the section ”Generation and Usage of Data”, empirical data acquired from cycling the samples in G1 was used to train multiple regression models in MATLAB.

Figure 4.1: *Aging Curves of G1*

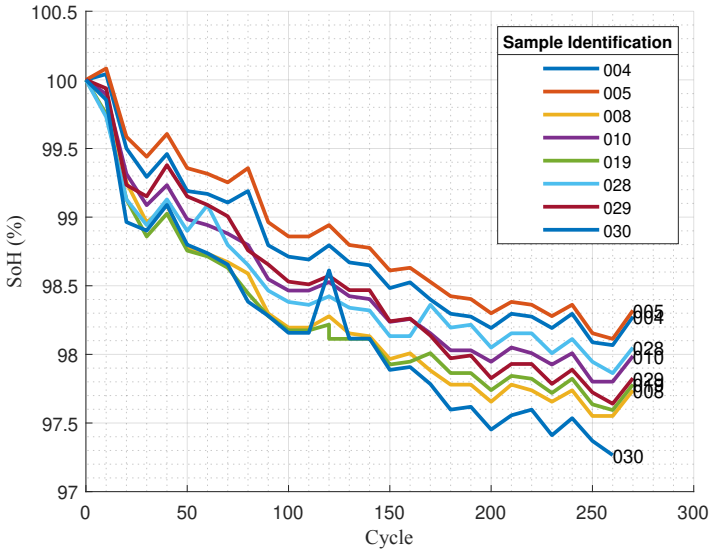

After evaluating the results, the best-fitting regression model for the detailed model

was identified as the ”Rational Quadratic Gaussian Process Regression” which achieved a root mean square error (RMSE) of 0.177. As illustrated in Fig. 4.2, the predicted SoH aligns closely with the measured SoH, following a near-perfect 1:1 ratio line. This indicates a strong correlation between the estimations and the actual measured values. The trained model was further validated using the data from the samples in G2 to confirm that the model is applicable to similar commercialized cells.

Figure 4.2: *Predicted Vs Actual SoH of G1*

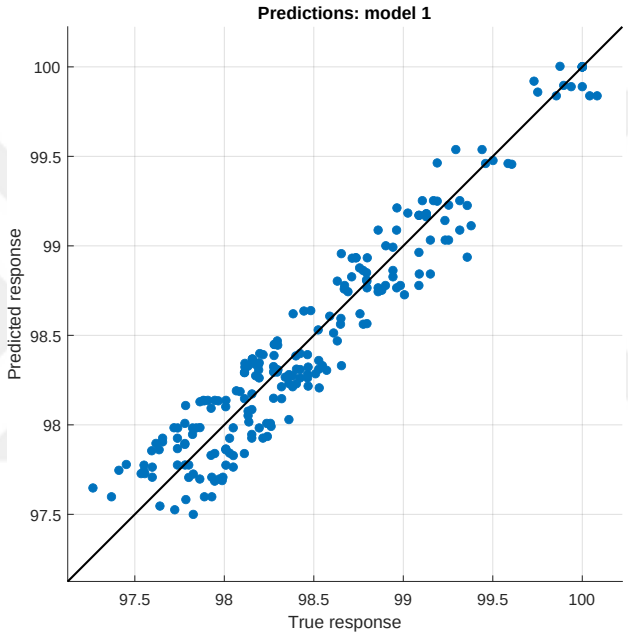

4.2 Sample Group G2

Cells assigned to G2 are used to validate detailed estimation model. Each cell of the group is put under aging test plan according to Fig. 3.2. During aging, key parameters of the cells are collected and then used to compare with the estimated SoH. Difference between predicted and measured SoH of each cells are shared in the following Figures 4.3, 4.4, 4.5, 4.6.

Figure 4.3: *Prediction vs Measured SoH of 003*

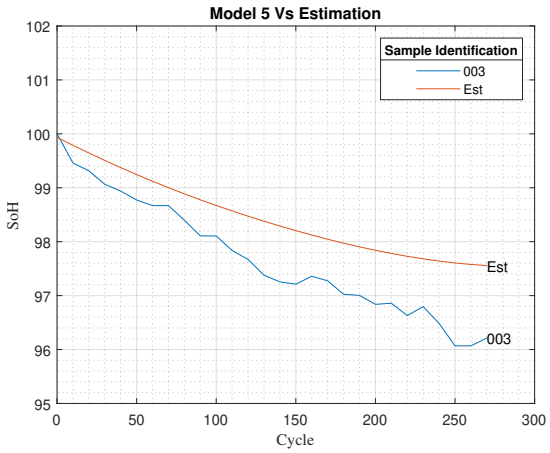

When prediction values and the measured values of SoH is used to observe the RMSE, SoH prediction of 003 is calculated as 0,864 which means that the average error when estimating the SoH is 0.864%. When compared with the rest of the estimation RMSE's, Cell 003's estimations has the biggest RMSE. When data of cell 009 is used to calculate RMSE of the prediction resulted with the RMSE of 0.550%.

Figure 4.4: *Prediction vs Measured SoH of 009*

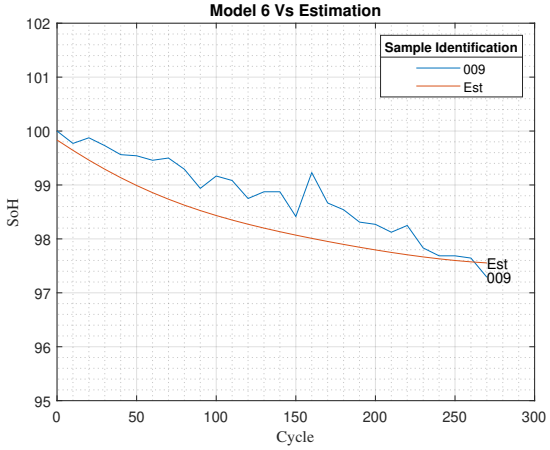

Lowest errors are observed at the predictions of cell 011. After calculation it is seen that the RMSE of cell 011 predictions is 0.291% overall. As explained in the first paragraph, predicted and the measured SoH are illustrated in Figure 4.5.

Figure 4.5: *Prediction vs Measured SoH of 011*

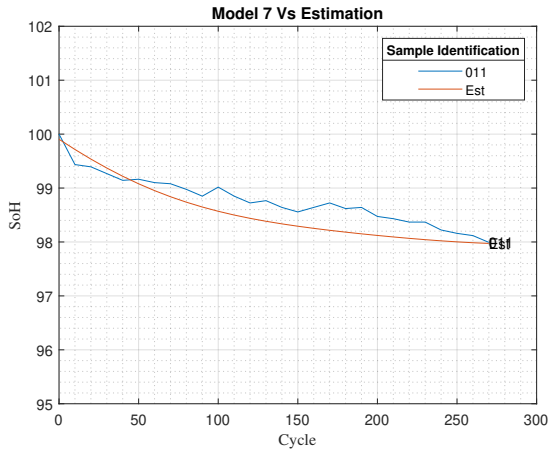

Similar to predictions of 011, RMSE is calculated as 0,348% for the predictions of cell 012. Errors between the predicted and measured SoH is illustrated in Figure 4.6.

Figure 4.6: *Prediction vs Measured SoH of 012*

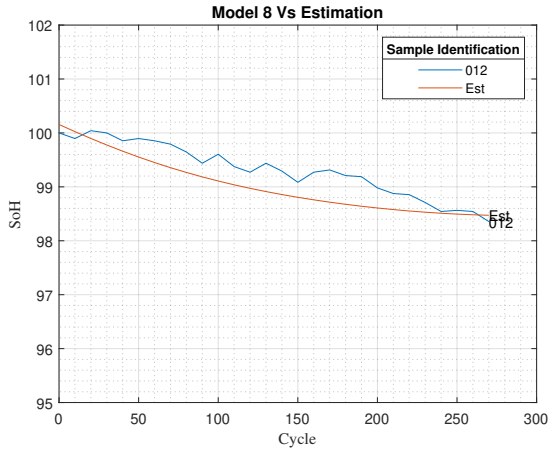

4.3 Sample Group G3

Cells of G3 are similar to the cells of G1 in terms of target which is to generate an estimation profile. As explained in section ”Generation and Usage of Data”, empirical data acquired from cycling the samples in G3 was again used to train multiple regression models in MATLAB. Simpler method generated by G3 samples requires completed cycle

numbers and the change of DCIR in percentage. Therefore, during testing cycle, SoH is tracked similar to G1 however instead of charging current and depth of discharge, DCIR of cells are tracked. In Figure 4.8(a), change of SoH is illustrated in terms of cycles. In Fig. 4.8(b) change of DCIR of G3 cells are illustrated. After evaluating the results, unlike G1; the best-fitting regression model for the detailed model was identified as the "Linear Regression Model," which achieved a RMSE of 0.316. As illustrated in Figure 4.2, the predicted SoH aligns closely with the measured SoH. The trained model was further validated using the data from the samples in G4 to confirm that the model is applicable to similar commercialized cells.

Figure 4.7: *Aging Curves and DCIR Behavior of G3 Samples*

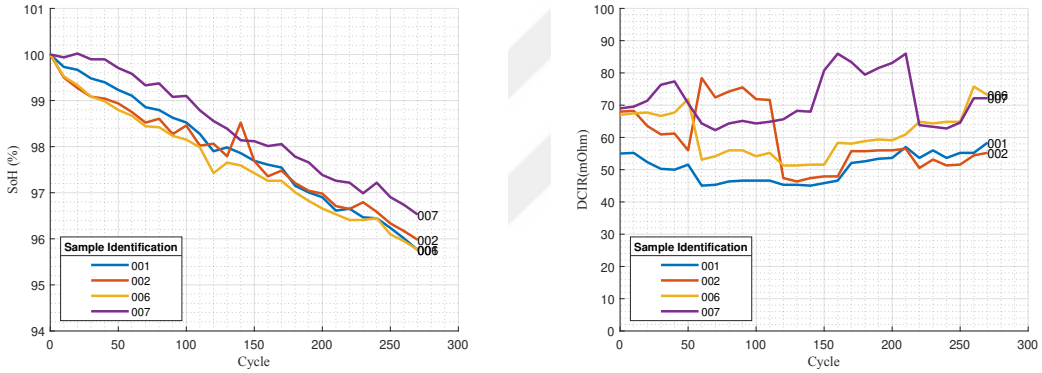

(a) Aging Curves of G3 Samples

(b) Change of DCIR in G3 Samples

Figure 4.8: *Predicted Vs Actual SoH of G3*

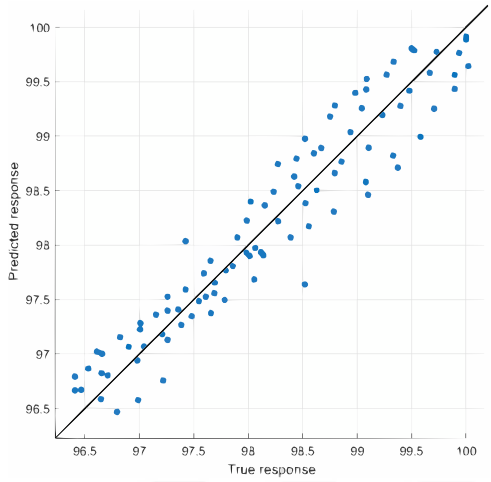

4.4 Sample Group G4

Cells assigned to G4 are used to validate simpler estimation model. Each cell of the group is put under aging test plan according to Figure 3.2. During aging, key parameters of the cells are collected and then used to compare with the estimated SoH. Difference between predicted and measured SoH of each cells are shared in the following Figures 4.9, 4.10, 4.11, 4.12.

Figure 4.9: *Prediction vs Measured SoH of 023*

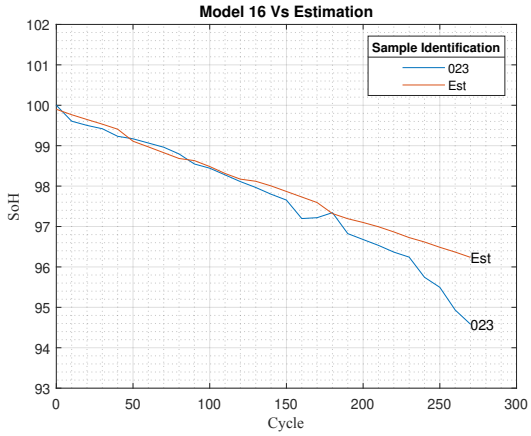

When prediction values and the measured values of SoH is used to observe the

error RMSE, SoH prediction of 023 is calculated as 0.5425 which means that the average error when estimating the SoH is 0.5425%. Similarly, data of cell 017 is used to calculate RMSE of the prediction resulting with the RMSE of 0.6009%.

Figure 4.10: *Prediction vs Measured SoH of 017*

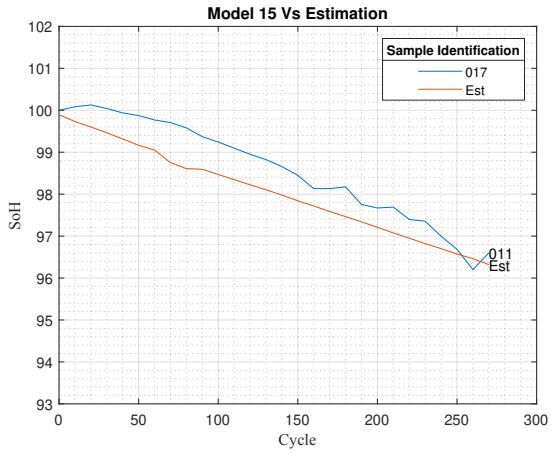

Lowest errors are observed at the predictions of cell 021. After calculation it is seen that the RMSE of cell 021 predictions is 0.3207% overall. As explained in the first paragraph, predicted and the measured SoH are illustrated in Figure 4.5.

Figure 4.11: *Prediction vs Measured SoH of 021*

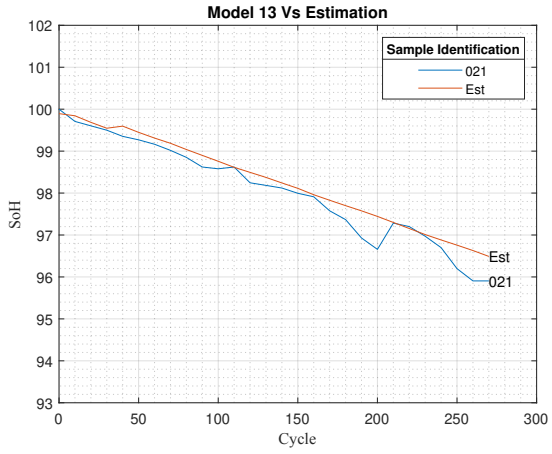

While the predictions of cell 021 being the most accurate; lowest accuracy is

observed at the predictions of 014. RMSE is calculated as 0.7815% for the predictions of cell 017. Errors between the predicted and measured SoH is illustrated in Figure 4.6.

Figure 4.12: *Prediction vs Measured SoH of 014*

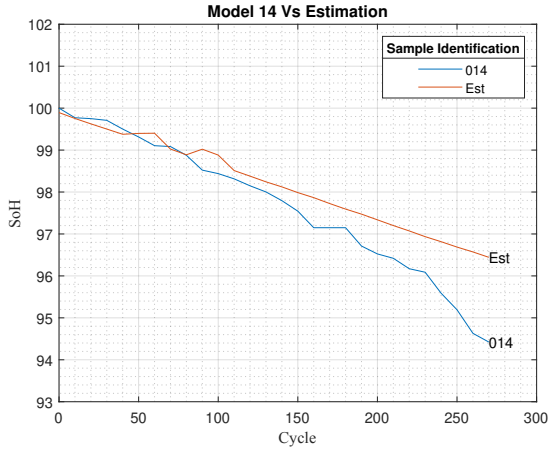

5. DISCUSSION

The primary focus of this study is to identify an optimal estimation method for determining the SoH of cells intended for second-life applications under stable, controlled conditions. In this chapter, we evaluate the test results for the cells, examining both the applicability and scalability of the proposed estimation methods in second-life scenarios. Each model demonstrates distinct strengths and limitations, which are analyzed here to assess their potential for practical implementation in large-scale applications.

5.1 Comparison of Estimations Derived From Sample Group G1 and Sample Group G3 for First and Second Life Applications

The detailed estimation model developed from sample group G1 and the simpler model from sample group G3 are each suited to different use cases for first and second life. The simpler model, which uses only cycle count and DCIR change as inputs, works well for specific second-life applications that have stable conditions, like constant charging and discharging profiles, set DoD, and steady temperatures. With fewer input requirements, it's easier to apply in scenarios with consistent operation, making it a practical choice for second-life applications focused on simpler management.

The detailed model, which uses cycle count, charging current, and DoD as inputs, can support applications with different current ratings, as long as those ratings remain constant within each application. This gives it more flexibility, allowing manufacturers to apply it across various products that need different current levels. For effective use, manufacturers can build a dataset from performance tests covering multiple steady-current profiles, helping the detailed model make accurate predictions across different product types.

In summary, each model has its own strengths. The simpler model is efficient for stable, predictable second-life applications, while the detailed model is better for flexible

applications that need more accurate predictions across a range of conditions. This comparison shows how each model serves different goals, balancing flexibility with the data needed for second-life use.

5.2 Compability of Estimation Model Generated From Sample Group G1 with Sample Group G2 Results

As outlined in section 4.1, the G1 detailed estimation model achieved an RMSE of 0.177 using the initial Rational Quadratic Gaussian Process Regression, indicating strong accuracy. Upon completion of aging tests, each validation sample was compared with its estimation curves. Despite the cells being commercially produced, performance differences are inherent. Manufacturers typically specify a minimum rated capacity to comply with standards, meaning some cells may exceed these specifications and perform better than others, which can introduce variability in the estimation model. To address this, each cell's unique initial capacity (zero-hour capacity) was used to calculate SoH rather than the rated capacity. However, this adjustment led to an SoH overshoot, particularly in cells with low DoD. Initial SoH levels of cells 004 and 005 showed similar overshoots, like cell 012; however, given the limited number of cells tested, such anomalies cannot be fully accounted for by the gaussian regression alone. Validation test results, shown in Table 5.1, have RMSE values ranging from 0.291% to 0,864%.

Table 5.1: *Summary of Sample Group G2's RMSE*

$Cell$	$RMSE$
003	0.864%
009	0.550%
011	0.291%
012	0.348%

Although validation tests show slightly higher estimation errors compared to the overall RMSE of sample group G1's results, achieving an SoH estimation within 1–4%

is satisfactory for secondary life applications of cells in static environments. These methods are designed for cost-effective, widely used products that lack high-level hardware and computational power found in grid systems or electric vehicles. Considering the consistency of both the generation and validation test results, this detailed estimation approach appears suitable for consumer products. Moreover, as battery recycling remains a challenge, implementing second-life applications could effectively extend the usability of cells and batteries, enhancing sustainability.

5.3 Compability of Estimation Model Generated From Sample Group G3 with Sample Group G4 Results

As outlined in section 4.2, the G3 simpler estimation model achieved an RMSE of 0.316 using linear regression, indicating strong but lower accuracy compared to the detailed estimation model. After completing aging tests, each validation sample was compared with its estimation curves. Despite the cells being commercially produced, inherent performance differences were observed, as discussed in section 5.2. Both cellfs from sample group G3 and G4 had SoH overshoot similar to the detailed model, with the initial SoH levels of cells 007 and 017 displaying comparable overshoots. However, unlike the detailed model, this overshoot did not significantly increase the RMSE, which resulted in a value of 0.6009% error. Validation test results, shown in Table 5.2, have RMSE values ranging from 0.3207% to 0.7815%.

Table 5.2: *Summary of Sample Group G4's RMSE*

$Cell$	$RMSE$
014	0.7815%
017	0.6009%
021	0.3207%
023	0.5425%

The findings suggest that while the simpler model works better for specific usage

scenarios, maintaining a stable connection with the cells is essential, particularly without utilizing permanent connection methods. If manufacturers wish to adjust the usage scenario, new tests with a sufficient number of samples must be conducted. An unstable connection may alter the DCIR when measured from the terminals, leading to estimation errors. As illustrated in Figure 4.8(b), potential measurement errors can arise from small changes in contact resistance within cell fixtures. Therefore, when considering the use of non-permanent cell holders for the final product to qualify for second-life applications, battery manufacturers must ensure a stable and rigid connection. Even the slightest change at the contact point on the cell surface can significantly impact the measured DCIR. Despite these small errors, the simpler model demonstrates promising estimation values.

5.4 Comparison Between Estimation Models of G1 & G3

When comparing the detailed estimation model (G1) with the simpler model (G3), several key differences and implications for second-life applications emerge. The detailed model, which incorporates charging current, DoD and cycle numbers as inputs, demonstrates high accuracy with an RMSE of 0.177. This flexibility allows manufacturers to utilize cells across various applications, even under different current ratings, although the current must remain stable. However, the detailed model's performance is affected by overshoots, particularly with certain cells, which may necessitate a larger number of tested samples to enhance its reliability. In contrast, the simpler model relies on fewer inputs—specifically, cycles and changes in DCIR resulting in a higher RMSE of 0.316. While this indicates lower accuracy, it can still effectively estimate the SoH in practical applications. Both models exhibit SoH overshoot; however, the simpler model does not increase the RMSE as significantly, maintaining a range of 0.3207% to 0.7815% in validation tests. Ultimately, the choice between the two models hinges on the manufacturer's

need for accuracy versus practicality, with the simpler model proving to be a viable option for estimating SoH in various second-life applications. A critical consideration for both models is the need for a rigid and stable connection during testing; any instability in the connection can introduce measurement errors, particularly in DCIR readings, thereby affecting the accuracy of the estimation.

6. CONCLUSIONS

This thesis presents a framework for estimating the SoH of Li ion cells to support their second life applications, incorporating non invasive analysis methods that prevent damage to cells and enable scalable, efficient SoH estimation. The study develops, validates, and compares two estimation models based on empirical data collected from various operational scenarios, including cycle count and a new control parameter, change of DCIR in terms of percentage, without direct observation of individual parameter effects for non permanently connected cells. By utilizing regression based modeling as a black box to assign parameter weights, the research provides a pathway for accurately estimating cell degradation patterns.

The primary objectives of this study involved researching battery assembly types, deciding best way to reuse based on batteries assembly types, developing predictive SoH estimation models, evaluating their accuracy across a range of cycling conditions, and investigating their applicability to second life usage scenarios. By building a non invasive second life framework, the study offers a valuable contribution to battery/cell analysis in contexts where preserving cell integrity is essential, especially for second-life applications where large scale individual testing is impractical. The findings underscore the potential to support second-life processes in various formats, including reuse of battery assemblies, disassembly of cells from batteries or other products, and repurposing cells in new battery configurations.

Key contributions to the literature include the definition and introduction of an entry level framework for the second life of cells, along with a non invasive second life model and dedicated SoH estimation models specifically designed for non permanent assembled cells and batteries. The study provides a comprehensive analysis of current battery manufacturing practices to illustrate the real battery life cycle, and it highlights scaling issues related to SoH estimation and second life applications while offering an

entry level solution. In addition, two SoH estimation models were developed by incorporating regression analysis to capture interactions among cycle count, DCIR, and usage parameters, thereby offering a comprehensive approach for predicting cell aging. These models were validated and compared under realistic usage profiles, with the results indicating that the detailed model offers a more reliable prediction of SoH. Furthermore, a non invasive approach to SoH estimation was demonstrated, providing a viable solution for assessing cell health without compromising cell integrity and thus supporting efficient and scalable second life applications. Finally, the research highlights various second life application options, including potential battery reuse in lower demand contexts, cell disassembly from multi cell configurations, and the creation of new assemblies from collected second life cells.

The study's emphasis on non invasive second life model aligns with industry needs for practical, scalable second life solutions. By enabling the reliable frame work of second life without physically altering or damaging cells, this approach supports a broader application of second life methods.

Future research could extend these models through additional studies focusing on enhanced data collection, integration with real world systems and validation, and comprehensive economical analysis. For instance, future studies should gather larger and more detailed datasets including longer cycles, discharge current, ambient temperature, and cell surface temperature to further refine the models. Moreover, this study lays the foundation for future research aimed at implementing and validating the proposed second life scenarios in real world applications. An essential aspect for future exploration is the economical analysis of the second life framework; while the framework has been developed with battery manufacturers in mind, the cost implications are crucial for determining industry adoption. As noted in this study, commercialized cells from a well known manufacturer were used to obtain realistic results, yet performance can vary significantly

between manufacturers due to differences in cell chemistry and manufacturing quality. Consequently, extending these studies to include cells from various brands would provide a more comprehensive understanding of model applicability and performance variability.

REFERENCES

[1] M. Berecibar, I. Gandiaga, I. Villarreal, N. Omar, J. Van Mierlo, and P. Van den Bossche, "Critical review of state of health estimation methods of li-ion batteries for real applications," *Renewable and Sustainable Energy Reviews*, vol. 56, no. C, pp. 572–587, 2016.

[2] R. Xiong, L. Li, and J. Tian, "Towards a smarter battery management system: A critical review on battery state of health monitoring methods," *Journal of Power Sources*, vol. 405, pp. 18–29, 2018.

[3] H. C. G. Zhou, F. Li, "Progress in flexible lithium batteries and future prospects," *Energy Environ. Sci.*, vol. 7, pp. 1307–1338, 2014.

[4] Q. L. S. C. S. F. Y. Wang, B. Liu, "Lithium and lithium ion batteries for applications in microelectronic devices: A review," *J. Power Sources,*, vol. 286, pp. 330–345, 2015.

[5] C. H. J.D Mackenzie, "Perspectives on energy storage for flexible electronic systems," *Proc. IEEE*, vol. 103, pp. 535–553, 2015.

[6] M. D. J. C. Xing Luo, Jihong Wang, "Overview of current development in electrical energy storage technologies and the application potential in power system operation," *Applied Energy*, vol. 137, pp. 511–536, 2015.

[7] J. T. L. G. Y. Naoki Nitta, Feixiang Wu, "Li-ion battery materials: present and future," *Materials Today*, vol. 18, pp. 252–264, 2015.

[8] D. C. M. F. L. T. Z. Y. Y. L. X. J. Y. G. YANG Jie, WANG Ting, "Overview of the modeling of lithium-ion batteries," *Energy Storage Science and Technology*, vol. 8, pp. 58–64, 2019.

[9] H. Z. Y. Z. W. T. Ran Li, Wenrui Li, "On-line estimation method of lithium-ion battery health status based on pso-svm," *Frontiers in Energy Research*, vol. 9, 2021.

[10] E. S. Tatiana Biagetti, "Automatic diagnostics and prognostics of energy conversion processes via knowledge-based systems," *Energy*, vol. 29, pp. 2553–2572, 2004.

[11] A. I. B. G. E. C. P. J. M. T. R. A. F. H. Yanyan Zhao, Oliver, "A review on battery market trends, second-life reuse, and recycling," *Circular Economy in Energy Storage Materials*, 2021.

[12] Q. L. Yu, Zhang, "Soh estimation method for lithium-ion battery based on discharge characteristics," *Internatial Journal of Electrochemical Science, Volume 17, Issue 7*, 2022.

[13] L. W. L. L. X. X. Z. G. L. Y. Chen, Hu, "State of health (soh) estimation and degradation modes analysis of pouch nmc532/graphite li-ion battery," *Journal of Power Sources*, 2021.

[14] A. H. A. M. M.A. Hannan, M.S.H. Lipu, "A review of lithium-ion battery state of charge estimation and management system in electric vehicle applications: Challenges and recommendations," *Renewable and Sustainable Energy Reviews*, vol. 78, 2017.

[15] G. X. Feng, "State-of-health estimation and remaining-useful-life prediction for lithium-ion battery using a hybrid data-driven method," *IEEE Transactions on Vehicular Technology*, 2020.

[16] X. L. M. P. Xiaosong Hu, Le Xu, "Battery lifetime prognosticsbattery lifetime prognostics," *Joule*, vol. 4, 2020.

[17] F. Z. B. Li, Liu, "Data-driven health estimation and lifetime prediction of lithium-ion batteries: A review," *Renewable and Sustainable Energy Reviews*, vol. 113, 2019.

[18] S. T. A. Stroe, Swierczynski, "Accelerated lifetime testing methodology for lifetime estimation of lithium-ion batteries used in augmented wind power plants," *IEEE Transactions on Industry Applications*, vol. 50, 2014.

[19] S. Y. Lall, Soni, "Soh modelling of li-ion coin cells subjected to varying c-rates, depths of charge, operating temperatures and custom charge profiles," *2021 20th IEEE Intersociety Conference on Thermal and Thermomechanical Phenomena in Electronic Systems (iTherm)*, 2021.

[20] S. Y. Lall, Soni, "Estimation of soh degradation of coin cells subjected to accelerated life cycling with randomized cycling depths and c-rates," *IEEE International Reliability Physics Symposium (IRPS)*, 2023.

[21] Zhang, "A new method for lithium-ion battery's soh estimation and rul prediction," *:13th IEEE Conference on Industrial Electronics and Applications (ICIEA)*, 2018.

[22] L. H. Teng, Chen, "Accurate and efficient soh estimation for retired batteries," *Energies 2023, 16, 1240.*, 2023.

[23] L. W. M. W. Lyu, Zhang, "Soh estimation of lithium-ion batteries based on fast time domain impedance spectroscopy," *:14th IEEE Conference on Industrial Electronics and Applications (ICIEA)*, 2019.

[24] C. S. S. Nobile, Vasta, "Estimation of soh for battery packs: A real-time mixed algorithm based on coulomb counting method and parameter-varying circuit modeling," *: 2020 IEEE 11th International Symposium on Power Electronics for Distributed Generation Systems (PEDG)*, 2020.